REPORT DOCUMENTATION PAGE

Form Approved
OMB NO. 0704-0188

1. AGENCY USE ONLY (Leave Blank)	2. REPORT DATE *Advanced Materials*, **18**, 2665–2678 (2006).	3. REPORT TYPE AND DATES COVERED Journal Reprint, September 2006

4. TITLE AND SUBTITLE
Introducing defects in 3D photonic crystals: State of the art

5. FUNDING NUMBERS
DAAD190310227

6. AUTHOR(S)
P. V. Braun, S. A. Pruzinsky, and F. Garcia-Santamaria

7. PERFORMING ORGANIZATION NAME(S) AND ADDRESS(ES)
University of Illinois-Urbana-Champaign
109 Coble Hall
801 S. Wright Street
Champaign, IL 618206242

8. PERFORMING ORGANIZATION REPORT NUMBER

9. SPONSORING / MONITORING AGENCY NAME(S) AND ADDRESS(ES)
U. S. Army Research Office
P.O. Box 12211
Research Triangle Park, NC 27709-2211

10. SPONSORING / MONITORING AGENCY REPORT NUMBER
45105.53-MS-MUR

11. SUPPLEMENTARY NOTES
The views, opinions and/or findings contained in this report are those of the author(s) and should not be construed as an official Department of the Army position, policy or decision, unless so designated by other documentation.

12 a. DISTRIBUTION / AVAILABILITY STATEMENT
Approved for public release; Government Rights

12 b. DISTRIBUTION CODE

13. ABSTRACT (Maximum 200 words)

3D photonic crystals (PhCs) and photonic bandgap (PBG) materials have attracted considerable scientific and technological interest. In order to provide functionality to PhCs, the introduction of controlled defects is necessary; the importance of defects in PhCs is comparable to that of dopants in semiconductors. Over the past few years, significant advances have been achieved through a diverse set of fabrication techniques. While for some routes to 3D PhCs, such as conventional lithography, the incorporation of defects is relatively straightforward; other methods, for example, selfassembly of colloidal crystals (CCs) or holography, require new external methods for defect incorporation. In this review, we will cover the state of the art in the design and fabrication of defects within 3D PhCs. The figure displays a fluorescence laser scanning confocal microscopy image of a y-splitter defect formed through two-photon polymerization within a CC.

14. SUBJECT TERMS

15. NUMBER OF PAGES
14

16. PRICE CODE

17. SECURITY CLASSIFICATION OR REPORT	18. SECURITY CLASSIFICATION ON THIS PAGE	19. SECURITY CLASSIFICATION OF ABSTRACT	20. LIMITATION OF ABSTRACT
UNCLASSIFIED	**UNCLASSIFIED**	**UNCLASSIFIED**	**UL**

DOI: 10.1002/adma.200600769

Introducing Defects in 3D Photonic Crystals: State of the Art**

By *Paul V. Braun*,* *Stephanie A. Rinne*,* and *Florencio García-Santamaría**

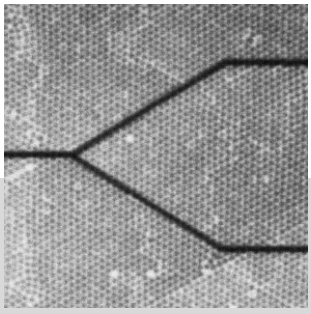

3D photonic crystals (PhCs) and photonic bandgap (PBG) materials have attracted considerable scientific and technological interest. In order to provide functionality to PhCs, the introduction of controlled defects is necessary; the importance of defects in PhCs is comparable to that of dopants in semiconductors. Over the past few years, significant advances have been achieved through a diverse set of fabrication techniques. While for some routes to 3D PhCs, such as conventional lithography, the incorporation of defects is relatively straightforward; other methods, for example, self-assembly of colloidal crystals (CCs) or holography, require new external methods for defect incorporation. In this review, we will cover the state of the art in the design and fabrication of defects within 3D PhCs. The figure displays a fluorescence laser scanning confocal microscopy image of a y-splitter defect formed through two-photon polymerization within a CC.

1. Introduction

Photonic crystals (PhCs) are materials that possess spatial periodicity in their dielectric constant on the order of the wavelength (λ) of light. These materials can strongly modulate light[1] and, with sufficient dielectric contrast and an appropriate geometry, may exhibit a photonic bandgap (PBG). This concept was first proposed in 1975 by Bykov[2] but remained relatively unknown until the seminal work of Yablonovitch[3] and John.[4] In a rough analogy to semiconductors, which possess an electronic bandgap, a PBG material prohibits the existence of photons with energies in the PBG. PhCs are naturally classified by the dimensionality of their periodicity, and in order to rigorously prevent the propagation of PBG frequencies in all directions, a 3D PhC with an omnidirectional, or complete PBG (cPBG) is required.

cPBG materials have been fabricated and well characterized for operation at microwave and radio frequencies, however, operation in the visible and IR requires the characteristic length scales of these structures to be scaled down by several orders of magnitude, necessitating 3D fabrication techniques capable of defining structures with sub-micrometer- to micrometer-scale periodicity and nanometer-scale resolution. Additionally, cPBG structures must be fabricated from optically transparent materials with a high dielectric constant. In the optical regime, there is a limited set of materials satisfying these conditions, largely ruling out organic and metallic materials, most oxides, and many semiconductor-based structures. Because of the materials restrictions and stringent 3D fabrication requirements, there are only a small, but growing, number of cPBG materials that have been constructed in the visible or IR. A review of PBG fabrication methods can be found in the literature.[5] The development of efficient, practical techniques amenable to the fabrication of cPBG materials operating in the visible to IR remains a vibrant area of research, with new approaches regularly being introduced in the literature.

[*] Prof. P. V. Braun, Dr. S. A. Rinne, Dr. F. García-Santamaría
Department of Materials Science and Engineering
Beckman Institute for Advanced Science and Technology and
Frederick Seitz Materials Research Laboratory
University of Illinois at Urbana-Champaign
1304 West Green St., Urbana, IL 61801 (USA)
E-mail: pbraun@uiuc.edu; sarinne@uiuc.edu; floren@uiuc.edu

[**] The authors thank the following for support: the U. S. Army Research Laboratory and the U. S. Army Research Office grant DAAD19-03-1-0227; the National Science Foundation; and the U.S. Department of Energy, Division of Materials Sciences grant DEFG02-91ER45439, through the Frederick Seitz Materials Research Laboratory at the University of Illinois at Urbana-Champaign.

Many applications have been identified for PhCs and PBG materials, including low-threshold lasers,[3] low-loss waveguides,[6–8] on-chip optical circuitry,[9] and fiber optics.[10,11] The majority of these applications not only require a PBG material, but also the precise, controlled incorporation of pre-engineered defects. These defects disrupt the periodicity of the crystal, creating optical states within the otherwise forbidden bandgap frequencies. Therefore, light coupling to these states can be localized within the defect regions and manipulated by engineering the defect geometry and placement. For example, a complicated 3D defect with sharp bend radii (ca. λ) may be engineered to guide light along its complex path without loss if defined within a cPBG material.[12] Similarly, point defects may be defined within PBG materials to create embedded optical cavities. Such cavities containing an emitting material could be used to inhibit spontaneous emission.

This review will focus on the incorporation of defects in 3D PhCs that operate at optical wavelengths and it is organized by the type of defect and the technique used to fabricate the PhC lattice. Defect fabrication techniques will be evaluated on their potential resolution, accuracy of registration with the underlying PhC lattice, flexibility in defining complicated embedded 3D structures, and their potential to incorporate materials that might impart additional functionality. If available, optical characterization and theoretical modeling of these de-

Paul V. Braun is an Associate Professor and Willett Faculty Scholar in Materials Science and Engineering, the Frederick Seitz Materials Research Laboratory, and the Beckman Institute for Advanced Science and Technology, at the University of Illinois at Urbana-Champaign (UIUC). Prof. Braun has authored four books or edited volumes, 55 publications, and multiple proceedings and abstracts. He is the recipient of a Beckman Young Investigator Award (2001), a 3M Nontenured Faculty Award, the 2002 Robert Lansing Hardy Award from TMS, given to one outstanding materials scientist each year, the Xerox Award for Faculty Research (2004), and multiple teaching awards. Professor Braun received his B.S. degree from Cornell University in 1993, and his Ph.D. in Materials Science and Engineering from UIUC in 1998, both in Materials Science and Engineering. Following a one year postdoctoral appointment at Bell Labs, Lucent Technologies, he joined the faculty at UIUC in 1999.

Stephanie Rinne (née Pruzinsky) was a National Science Foundation (NSF) graduate fellow in the Department of Materials Science and Engineering at the UIUC. Her Ph.D. thesis work in Prof. Braun's group focused on the two-photon polymerization and optical characterization of embedded features within self-assembled photonic crystals. Upon completion of her Ph.D. Stephanie began a postdoctoral fellowship at the Beckman Institute for Advanced Science and Technology at UIUC in July, where she is working in the area of biomedical imaging. Stephanie received her B.S. in Materials Science and Engineering at Rensselaer Polytechnic Institute in 2000. As an undergraduate, she participated in NSF summer research projects in surface and interfacial science at the University of Massachusetts at Amherst and Stanford University.

Florencio García-Santamaría is a postdoctoral scientist in Prof. Braun's group in the Department of Materials Science and Engineering at UIUC. His major research interests have been the optical characterization and fabrication of 3D photonic crystals. Florencio received his B.S. degree in theoretical physics from the Universidad Autonoma de Madrid (UAM) in 1998. His doctorate was conducted at the Institute of Materials Science of Madrid (ICMM-CSIC) where he investigated self-assembled artificial opals and developed a method to fabricate photonic crystals with diamond symmetry, working with Profs. Cefe Lopez and Francisco Meseguer. He obtained his M.S. (2001) and Ph.D. (2003) degrees from the UAM; his work as a graduate student was named the 'Outstanding dissertation of 2003–2004' at the same university.

ADVANCED MATERIALS

fects will be included. We categorize defects in two types: intrinsic and extrinsic. In the former case defect formation does not require any special processing aside from that needed to form the PhC itself (e.g., conventional photolithography and direct writing). In the latter case, the PhC fabrication technique lacks an inherent means for the incorporation of defects (e.g., holographic lithography and self-assembly) and they are introduced before or after formation of the PhC.

2. Defects in 2D PhCs

Initially 2D PhCs did not generate as much excitement as their 3D counterparts since they cannot rigorously confine light in all dimensions. However, due to the substantial fabrication and modeling advantages in two dimensions, the experimental and theoretical work on defect-containing 2D PhCs is significantly advanced over that on 3D PhCs. The confinement of light within the plane of a 2D PhC is achieved by sandwiching the 2D PhC between Bragg reflectors,[13] 3D PhCs,[14] or lower-index materials, including air, to utilize total internal reflection.[15]

2D PhCs that operate at optical wavelengths have a periodicity of ca. 100 nm–1 μm with feature tolerances in the nanometer range. Typical 2D PhCs consist of triangular arrays of air cylinders in a dielectric material, as this geometry can yield a 2D PBG for any polarization, provided the dielectric has a refractive index over 2.7.[16] With state of the art lithography,[13,17] followed by reactive-ion or electrochemical etching, high-resolution 2D PhCs can be defined in high-refractive-index materials including silicon and III-V semiconductors.

The addition of defects to these structures is carried out simultaneously with the fabrication of the 2D PhC, affording excellent registration between the defects and the lattice. By removing a line of cylinders from the initial design, linear waveguides can be introduced into a 2D PBG material (Fig. 1).[18,19] Point defects, formed by removing or reshaping air cylinders, serve as resonant cavities that can trap photons of certain frequencies.[18] Through proper engineering, very high Q cavities (up to 600 000) have been reported (Fig. 2).[20] Furthermore, various defect designs have been proposed and, in some cases, realized for low-loss waveguides containing sharp bends,[8] channel drop filters,[21,22] and T-shaped branches.[23] By introducing active materials (e.g., quantum wells or dots) in the design of the PhC the possibility of using point defects as resonant cavities for lasing action has also been demonstrated.[24–26]

3. Defects in 3D PhCs

Although 2D PhCs containing exquisitely designed defects have exhibited powerful optical properties, it remains true that

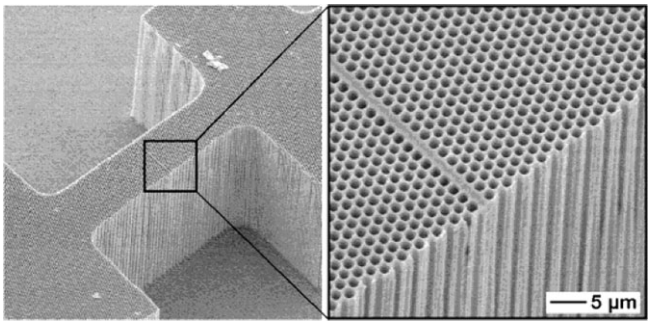

Figure 1. Scanning electron microscopy (SEM) image of a macroporous silicon 2D PhC containing a line defect. The pore pitch is 1.5 μm and the PhC is 100 μm deep. Reproduced from [19].

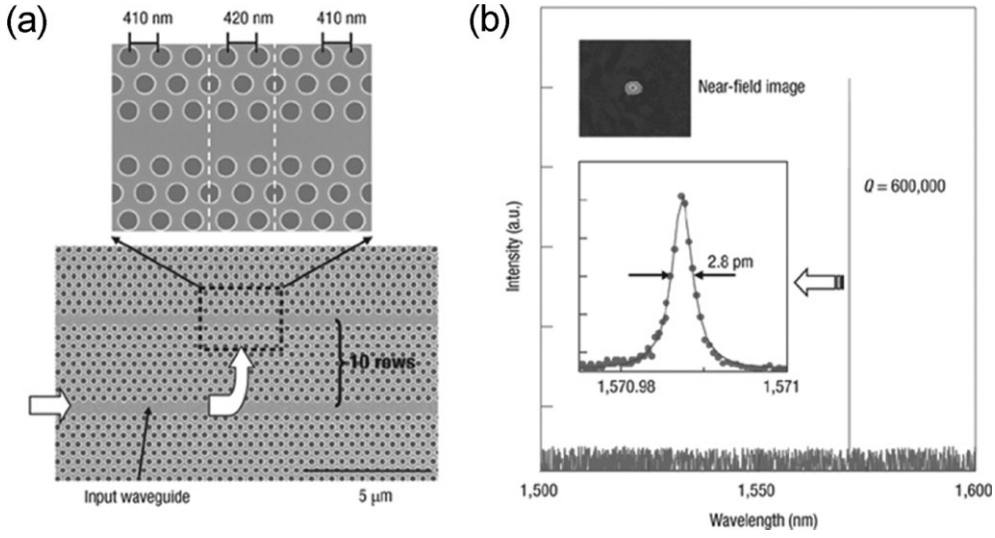

Figure 2. a) SEM image and b) spectra from a photonic double heterostructure nanocavity. The insets in (b) show a near-field image and high-resolution spectrum of the resonance. A linewidth of 2.8 pm and a Q-factor of 600 000 were observed. Reproduced with permission from [20]. Copyright 2005 Macmillan.

complete confinement of light can only be achieved by extending the PBG into the third dimension. From a fabrication and materials standpoint, 3D systems containing defined defect structures present a difficult set of challenges. For a cPBG at optical wavelengths, a high-resolution 3D fabrication technique and high dielectric constant materials are required, significantly limiting both possible materials and processing routes. Still, several processing routes to cPBG materials have been identified. Those that are amenable to defect fabrication will be covered in this section. Important considerations will be discussed, including potential resolution, accuracy of defect registration with the PhC lattice, ability to define complicated structures, and potential for incorporation of materials with advanced functionalities. Although still limited, optical characterization and theoretical modeling of these defects will also be reviewed.

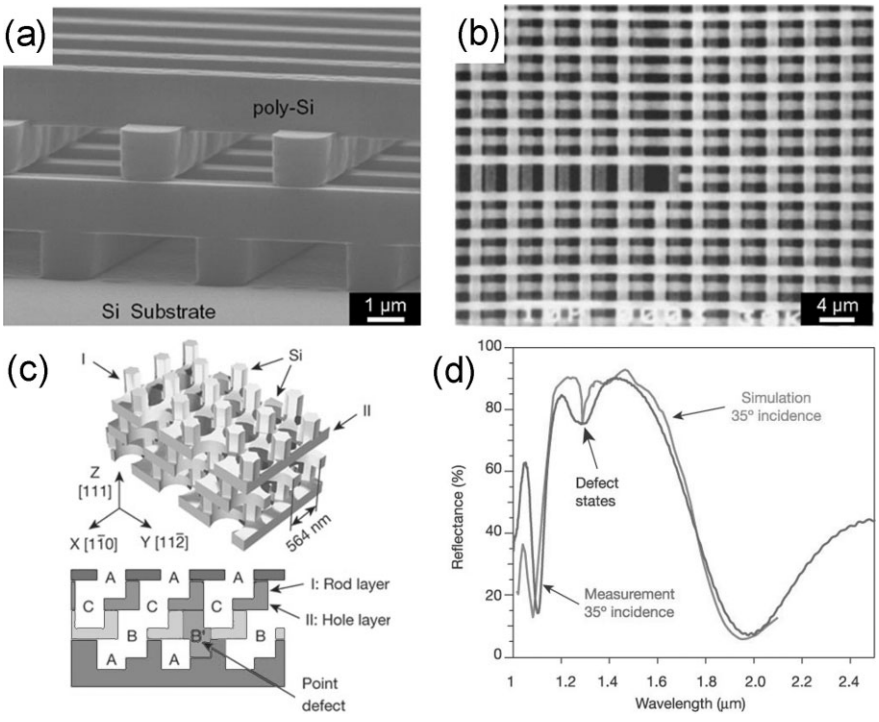

Figure 3. SEM images: a,b) side and top views of 3D PhCs built using conventional lithographic techniques ((a) reproduced with permission from [30]. Copyright 1998 Macmillan). b) The structure contains a sharp bend defect formed by leaving out rod portions during PhC fabrication. Reproduced with permission from [12]. Copyright 2000 AAAS. c) Schematic of a PhC containing point defects fabricated using similar techniques. d) Simulated and measured optical spectra obtained from the structure in (c); the defect state can be observed in both. Reproduced with permission from [31]. Copyright 2004 Macmillan.

3.1. Intrinsic Defects

3.1.1. Conventional Lithography

As the microelectronics industry has demonstrated, top-down lithography can create extraordinarily complex multilayer structures. Such layer-by-layer processing routes have now been exploited to create 3D PBG materials containing defined defect structures. On one hand, lithographic approaches have a number of shortcomings, from cost and practical limitations to the number of layers. For example, forming multilayer structures is tedious and difficult, requiring state-of-the-art processing equipment to overcome layer-to-layer registration issues. On the other hand, the infrastructure for lithographic approaches is extraordinarily well developed and, for some device applications, will probably be the method of choice for integrating 3D PCs with microelectronics.

The lithographic methods reported in the literature follow conventional 2D lithography and pattern-transfer techniques, and vary primarily in the procedure used to stack the multiple layers to create a 3D PhC (Fig. 3). Lithographic approaches are highly suitable for forming woodpile structures consisting of high-dielectric-constant rods assembled such that the contact points form a diamond lattice.[27] Noda and co-workers developed a 'wafer-fusion' method in which multiple layers are created on separate substrates and then aligned and fused together.[28] Leaving one or more rods out of the original pattern yields defects in the final 3D structure, for example, waveguide structures with sharp bends (Fig. 3b).[12] Transmission and reflection through such a bend was simulated through a finite difference time domain (FDTD) method.[29] The layer-by-layer approach pioneered by Lin et al. follows a classical device-fabrication process with repeated cycles of photolithography, wet and dry etching, chemical mechanical planarization, and sequential growth of SiN, Si, and SiO_2 thin films (Fig. 3a).[30] Following a related layer-by-layer procedure, Qi et al. successfully fabricated a 3D cPBG structure containing defined point defects (Fig. 3c).[31] Optical characterization showed the presence of defect states in agreement with theoretical simulations performed with a FDTD method[32] (Fig. 3d).

3.1.2. Electrochemical Etching

The formation of periodic arrays of micrometer-sized pores in n-type silicon through anodic etching[33] is an approach that has greatly advanced over the past decade and now enables the fabrication of Si-based 3D PhCs containing defined defects (Fig. 4). A substrate is first patterned with pyramidal pits through standard lithography followed by an isotropic wet etch. When the substrate is then placed in a HF acid solution

ADVANCED MATERIALS

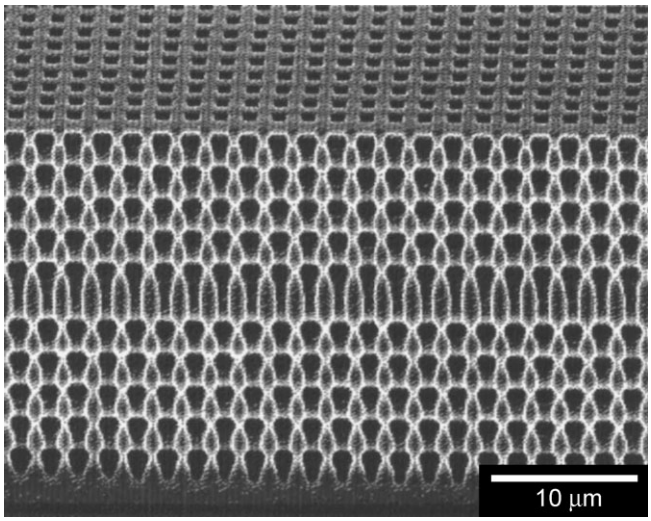

Figure 4. SEM side view image of a 3D PhC containing a planar defect fabricated by electrochemical etching. The defect has a width of 2.65 μm. Reproduced with permission from G. Mertens [39]. Copyright 2005 American Institute of Physics.

under an electrical bias, the enhanced current density at the tips of the pyramidal pits drives selective etching and propagates cylindrical holes through the substrate creating a 2D structure.[34] The method can be used to create 3D PhCs by modulating the light intensity during the etching with HF, varying the number of charge carriers which in turn modifies the dissolution of the Si. Thus, by modulating the illumination intensity, the internal microstructure, and thus local refractive index of the sample is controlled.[35–37]

This fabrication technique presents several advantages, perhaps the most significant of which is that the structure is formed from silicon, which has a high refractive index and is very well understood. There is the possibility for excellent control of the pore shape,[38] since the structure in the *z*-axis can be controlled independently of the other two axes. This feature makes the introduction of planar defects trivial since the structure in the *z*-axis is directly controlled by the illumination intensity (Fig. 4).[39] Also, linear defects normal to the surface are possible by modifying the initial pattern of the pyramidal pits. There are two significant shortcomings with this fabrication technique. First, the introduction of arbitrarily shaped defects presents an unresolved problem. Second, structures created this way show at best a very narrow cPBG[40] unless the process is combined with focused-ion-beam milling of channels,[41] which significantly reduces the simplicity of this method.

3.1.3. Glancing Angle Deposition

Glancing angle deposition (GLAD) is a relatively new technique amenable to the large-area microfabrication of 3D tetragonal square spiral PhCs,[42] structures which are theoretically capable of possessing a large and robust cPBG.[43,44] GLAD has been used to grow materials of interest for PhCs, including SiO_2, Si, Ge, TiO_2, and MgF_2. First, a flat substrate is patterned with a regular array of short seed posts via electron-beam (e-beam) or photolithography. Then, the substrate is exposed to a collimated vapor flux at a large incident angle, such that self-shadowing occurs during nucleation. Through shadowing and the limited adatom surface diffusion, nucleation and growth only occur on the top surface of the seed posts and oriented pillars emerge and grow toward the source of the incident vapor flux. By appropriately rotating the substrate during deposition, the growth and shape of these structures can be controlled, enabling the growth of circular, square, or polygonal spirals and the incorporation of embedded planar twist and spacing layer defects (Fig. 5).[45] Additionally, by eliminating points or lines in the initial seed pattern, silicon or air 2D point or line defects that extend through the thickness of the crystal have been defined.[46,47] Photonic bandstructure calculations have been performed for homogeneous 3D GLAD structures,[43,44] however, there is only limited optical characterization of either homogeneous and defect-containing GLAD structures. Transmission simulations have been performed on heterostructures composed of two tetragonal square spiral PhCs that sandwich a 2D PhC containing point and line defects.[14] The optical properties of ambichiral TiO_2 thin films with various polygonal helices have been interrogated. By comparing right- and left-handed circularly polarized transmitted light, the defect mode arising from an embedded twist layer defect was identified.[45] Although considerable work remains, and complex arbitrary embedded defects can not be directly formed by GLAD, for applications that require only

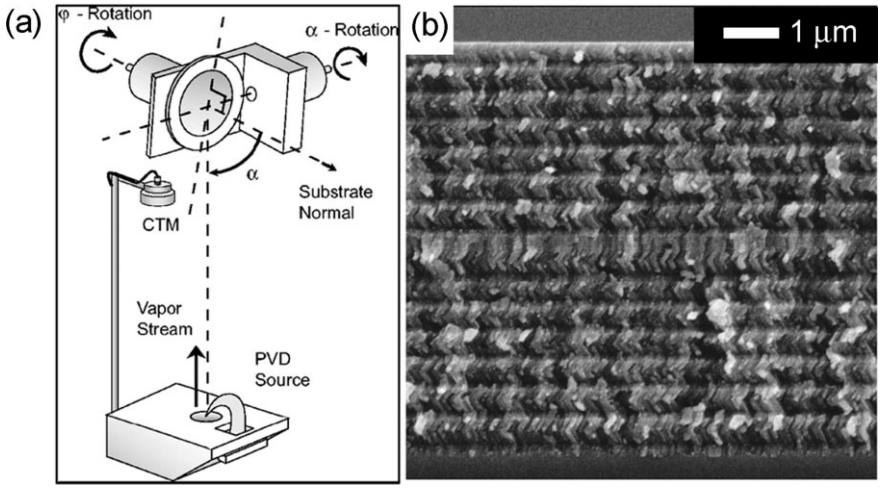

Figure 5. a) GLAD schematic. b) SEM side view image of a 3D PhC containing a 150 nm planar defect fabricated with GLAD. Reproduced with permission from A. C. van Popta [45]. Copyright 2005 American Institute of Physics.

simple twist, planar, or straight-line defects, GLAD may enable the rapid, and relatively low cost, fabrication of PhC structures over large areas.

3.1.4. Micromanipulation

Micromanipulation is an intriguing approach for the creation of nearly arbitrary 3D structures without the limitations of conventional lithography. Here, the PhC is built in a completely serial fashion from building blocks. For PhCs operating in the visible or near-IR regime the building blocks need to contain sub-micrometer features, and thus the use of optical tweezers or high-resolution robots attached to scanning electron or optical microscopes are ideal candidates for manipulating the building blocks.

Through the use of a nanorobot,[48] the first diamond structure formed out of colloidal microspheres was fabricated (Fig. 6a).[49] A glass probe nanomanipulator was first used to assemble polystyrene and silica microspheres into a body-centered structure; subsequent removal of the sacrificial polystyrene spheres led to a diamond structure of touching silica microspheres.[50] Through the appropriate placement of polystyrene microspheres, point defects could be embedded into the resulting structure. The same nanorobot was also used to fabricate woodpile structures presenting a cPBG (Fig. 6b).[51] Individual InP plates were fabricated by conventional integrated circuit processing, and then robotically stacked and aligned with the nanorobot to form structures of up to 20 layers. An advantage of using microfabricated InP plates over microspheres is that the structure was built one layer at a time rather than one particle at a time. The inclusion of defects was straightforward, simply requiring that one of the plates contained a pre-designed defect. Transmission spectra at varying angles were taken from an eight-layer structure containing an embedded defect formed by varying the pitch within two of the central layers. Comparison to calculations suggested that a resonant guided mode was being excited and transmitted through the sample.

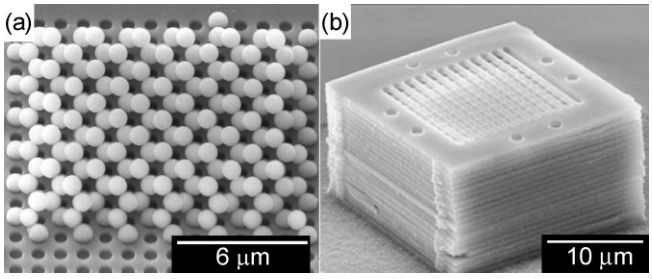

Figure 6. SEM image of PhCs fabricated with the aid of a nanorobot. a) Top view of a diamond structure of 1 μm silica colloids. Reproduced from [49]. b) Side view of a layer-by-layer structure. Reproduced with permission from [51]. Copyright 2003 Macmillan.

Laser optical trapping has not yet been used to create PhC-containing defects, but the potential is certainly present. Through optical trapping it is now possible to concurrently manipulate 3D arrays of colloidal microspheres.[52] Introduction of defects should be possible by simple modification of the trap array. Unfortunately, since this method requires a liquid medium and the traps cannot be allowed to overlap, it will be difficult to directly form close-packed, mechanically stable structures that retain their structure upon solvent removal. Perhaps, through new chemistries and assembly routes, it will become possible to create structures that can survive the drying process. To date, monolayers containing limited numbers of colloids have been formed through optical trapping followed by supercritical drying.[53]

Despite the many advances in optical trapping and robotics, including automatic image recognition[54] that will eventually improve and accelerate the process of fabrication, the use of micromanipulation assembly techniques seems to be restricted to small samples for scientific research.

3.1.5. Direct Writing

Direct writing of PhCs has been growing in interest due to both the ease of incorporation of defects, and a number of recent successes in 3D PhCs, including promising optical spectroscopy.[55,56] In principle, direct writing involves nothing more than converting a 3D computer aided design into a target material. Because the required dimensions are on the micrometer scale, traditional fabrication techniques, such as rapid prototyping, are not suitable and new approaches have been required. The most promising to date appear to be robotic ink writing[55,57,58] and laser writing by two-photon polymerization (TPP)[56, 59] (Fig. 7).

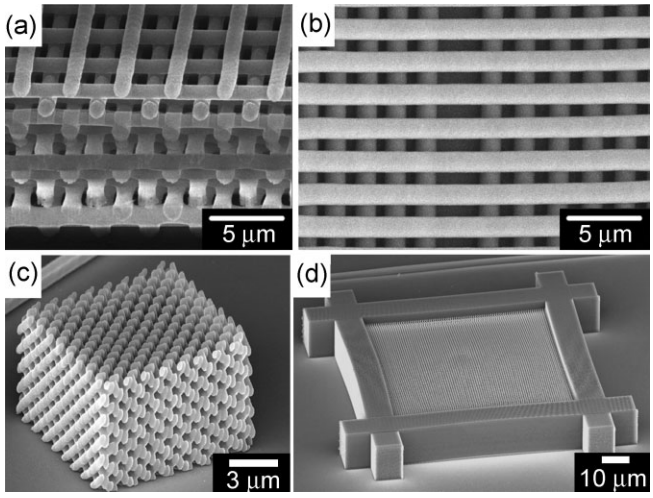

Figure 7. SEM images of PhCs fabricated by direct writing. a,b) Layer-by-layer structures created by ink-polymer writing [55, 58]; b) shows a linear defect from a missing rod; c,d) Slanted-pore and layer-by-layer structures, respectively, fabricated using TPP [78, 79]. (a) reproduced from [55], (b) courtesy of G. Gratson and J. Lewis, (c) reproduced with permission from Markus Deubel [79]. Copyright 2004 American Institute of Physics. (d) Reproduced with permission from [78]. Copyright 2004 Macmillan.

ADVANCED MATERIALS

Robotic ink writing consists of the fabrication of 3D microperiodic polymer scaffolds via direct-write assembly of a concentrated engineered polyelectrolyte ink that is extruded through a micrometer-diameter orifice.[60] If the ink rheology is properly designed, the deposited filaments maintain their cylindrical shape while spanning unsupported regions in the structure, yet adhere to both the substrate and the underlying layers. By means of this method, layer-by-layer[27] and woodpile[61] structures have been obtained.[55] The introduction of line defects can be easily achieved by modifying the computer design to move or remove individual lines (Fig. 7b). To date, the minimum rod diameter is ca. 1 μm and consequently the stop band lies between 3 and 5 μm. As is the case for PhCs made of polymers, the refractive-index contrast is not sufficient to generate a cPBG, so conversion of the polymer template to a high-refractive-index material is necessary. In a recent publication we demonstrated this conversion and characterized the resulting optical properties.[55] Theoretical and experimental optical studies on structures containing defects are yet to be performed.

Direct laser writing through multiphoton polymerization (MPP) is another powerful route to 3D fabrication. MPP was first developed by Strickler and Webb,[62] and has now been used to create a range of high-resolution 3D free-form structures, including microchannels,[63–65] cantilevers,[66–68] microgears,[69,70] sub-micrometer oscillators,[71] hydrophobic atomic force microscopy tips,[72] and PhCs.[59,67,73–81] Briefly, MPP utilizes the nonlinear nature of the multiphoton excitation process to only excite dye molecules in a very small volume around the focal point, with dimensions on the order of the resolution limit. These excited dye molecules locally initiate a polymerization. By scanning this localized excitation throughout a defined volume, a monomer can be polymerized into a robust intricate 3D polymer structure. This technique has also been used to write embedded features within holographic and self-assembled PhCs, see Sections 3.2.1 and 3.2.3, respectively. In most cases, MPP is a two-photon process, in which case we will refer to it as TPP.

TPP is a promising, flexible 3D fabrication technique that can be used to form both the PhC and, in principle, to embed arbitrarily complex defects. To date, PhC structures with layer-by-layer and slanted pore[82] geometries, presenting stop bands in the IR, have been fabricated (Fig. 7c and d).[59,78,79] Similar to robotic ink writing, the PhC is often fabricated in a polymer, and thus a similar replication approach is necessary to create a high-refractive-index contrast structure.[56] Alternatively, there are certain high-refractive-index chalcogenide glasses such as As_2S_3 that undergo solubility changes upon exposure to light and are therefore amenable to direct laser writing.[83] To date, there are no reports of optically active defects incorporated within TPP PhCs, however the process is straightforward.

3.2. Extrinsic Defects

3.2.1. Holographic Lithography

The concept of holographic lithography for PhC fabrication was first demonstrated by Berger et al. and is deceptively simple.[84] Inherently, it consists of recording the hologram created by the interference of multiple beams of light into a photoresist. Their first holographic PhC was a 2D triangular lattice obtained from the interference of three beams in a photoresist; the structure was subsequently replicated in GaAs. In holographic lithography, the minimum number of beams required to form an n-dimensional lattice is $n+1$, thus four beams were required to obtain the first 3D PhC with this technique.[85] The photoresist used in that study, and in most subsequent studies, was SU-8, a resist that has proven to be very useful due to its low intrinsic absorption and capability for forming sub-micrometer features.[86]

There are two key reasons why holographic lithography has the potential to become a leading method for 3D PhC fabrication. First, holography is highly amenable for large-scale production. Second, addition of optically active defects into the photoresist prior to development via laser direct writing is possible. The direct writing of features in holographic PhCs has now been demonstrated in both 2D[87] and 3D[88] structures (Fig. 8). To date, the optical properties of defects in holographically defined PhCs have not been studied, but this is likely to happen soon.

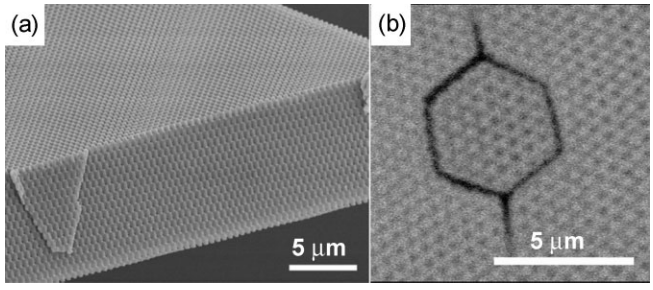

Figure 8. a) SEM image of PhCs fabricated using holographic lithography. b) Confocal microscope image of a feature embedded within the PhC written using TPP. Reproduced from [88].

There remain, however, several serious issues before the potential of holographic structures can be realized. The optical properties of 3D PhCs formed via holography are weaker than expected for reasons that are not obvious. There are only limited reports on the optical response of these structures[89] and although a direct comparison is difficult, to date, it appears that colloidal crystals (CCs) present better optical properties. The optical response of holographic structures could be improved by better lasers, photoresists, and processing param-

eters, but these improvements are not trivial. These issues become even more important as the number of interfering beams is increased to form more complex structures (e.g., diamond or chiral lattices).[90,91] An equally significant issue is that the refractive indices of common photoresists are too low to open a cPBG, regardless of the structure, thus, replicating the structures with high-refractive-index materials is essential. Advances in templating silicon with polymeric structures[55,56] indicate possible routes to create structures with enhanced refractive-index contrast. Also, very recently, Summers and coworkers[92] demonstrated the use of atomic layer deposition to replicate the structure of a holographic PC into TiO_2, a high-refractive-index material which is transparent in the visible region. Finally, since the exposure wavelength is directly proportional to the lattice parameter of the crystal, the chemistry of the photoinitiating system may need to be changed to tune the spectral position of the optical features. Although possible, this not a trivial task.[93] Even given these issues, holographic lithography coupled with direct laser writing is certainly an area of great potential.

A variant to holographic lithography in which the interference is created from a phase mask, as opposed to multiple beam interference, was demonstrated by Rogers and co-workers.[94] The phase mask is first defined in a 'master', fabricated through photolithography. This master is used to create a poly(dimethylsiloxane) (PDMS) flexible phase mask. The PDMS phase mask is placed in direct contact with the surface of a photoresist (SU-8) and illuminated with UV light, resulting in a complex 3D intensity distribution in the photoresist. Apart from the simplicity of this method, a very interesting feature of this fabrication technique is that it allows the introduction of both intrinsic and extrinsic defects. The former are obtained by creating defects in the original 2D master template.[94] It should be possible to form the latter via direct laser writing, as demonstrated in PhCs obtained by multibeam holographic lithography. Optical characterization of these structures has yet to be published.

3.2.2. X-Ray Lithography, Electroforming, Molding (LIGA)

LIGA is a deep-etch X-ray lithography microfabrication process which combines X-ray lithography, electrodeposition, and/or molding to circumvent the layer-to-layer registration and multistep processing issues found in conventional layer-by-layer lithographic approaches.[95,96] Through LIGA, high-aspect-ratio PhCs up to six crystal periods thick have been fabricated with sub-micrometer precision and low surface roughness. Synchrotron-based deep X-rays are used to expose poly(methyl methacrylate) (PMMA) through a patterned absorber mask. The exposed PMMA is removed, and the resulting structure can serve as a mold that is filled by electrodeposition or casting, forming a template of the PMMA mold in metal, ceramic, or composites.[97]

This technique enabled micrometer-scale fabrication of inverse Yablonovite[98] or "three cylinder" structures.[99] PMMA was exposed through a triangular array of holes via three tilted X-ray irradiations at 35° from the substrate normal and with a 120° rotation between exposures. Since the refractive index of PMMA is insufficient to open a cPBG, the interstitial space was filled with TiO_2 or metals.[97] Transmission and reflection spectra revealed the presence of a stop band at 2.4 μm, which is in agreement with transfer matrix method simulations. Defects can be incorporated into these structures via multiple exposure and multilayer resist schemes (Fig. 9).[100–102] Additional X-ray or e-beam exposures have been proposed for the definition of 2D defects in one layer of a multilayer resist, possibly enabling the incorporation of a plane of embedded 2D defects within PBG structures fabricated using LIGA.[100,102] The fact that synchrotron radiation is required, coupled with issues in uniformity for sub-micrometer structures, probably limits the general applicability of LIGA for PhCs operating at longer wavelengths.

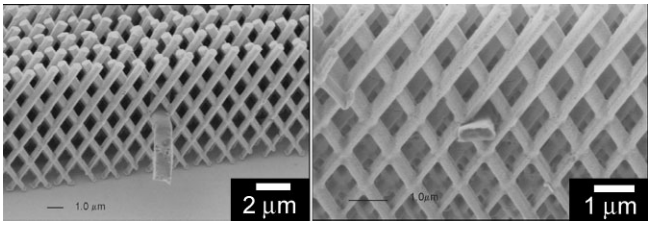

Figure 9. SEM image of metallic Yablonovite structures fabricated using LIGA. Linear resist-based defects can be seen within the structure. Reproduced with permission from [102]. Copyright 2005 IOP Publishing.

3.2.3. Colloidal Self-Assembly

Self-assembled CCs have been widely studied as routes to PhCs and PBG materials, in substantial part due to their ease of fabrication and low cost, but also due to their excellent optical properties. Typical colloidal PhCs consist of 3D face-centered cubic (fcc) arrays, self-assembled from highly monodisperse silica or polystyrene microspheres with diameters ranging from ca. 200 nm to 2 μm.[103] Most early research focused on improving CC quality and inverting them in high-refractive-index materials.[104] This is necessary because only a high-refractive-index contrast inverse-fcc geometry can possess a cPBG.[105] To utilize CCs for most cPBG applications, it is additionally necessary to incorporate designed defects within them. Since the controlled addition of well-defined intrinsic defects is not compatible with the self-assembly process, the viability of CCs for many PBG-based applications relies on a compatible external-defect fabrication technique. Substantial strides have been made over the last five years in the development of novel processes for the incorporation of point, linear, planar, and 3D defects within self-assembled PhCs.

Substitutional Doping: Although well-defined defects in CCs may have the greatest long-term potential, significant strides in understanding the impact of defects can be determined through the random placement of defects. The first intentional incorporation of optical defect states in a CC was ac-

ADVANCED MATERIALS

complished intrinsically via substitutional doping. Watson and co-workers doped colloidal suspensions with microspheres of different sizes or dielectric constants, and used this mixture to grow CCs with substitutional impurities.[106] Near-IR transmission spectroscopy was used to probe the optical properties of the wet crystals doped with both donor and acceptor impurities. Defect modes as well as a significant widening of the optical stop band were observed (Fig. 10). Spectra simulated using the transfer matrix method[107] qualitatively agreed with experimental results, though a quantitative comparison was not possible. Another doping study by Gates and Xia and later by Lopez and co-workers observed a reduction in attenuation of transmittance within the optical stopband with increas-

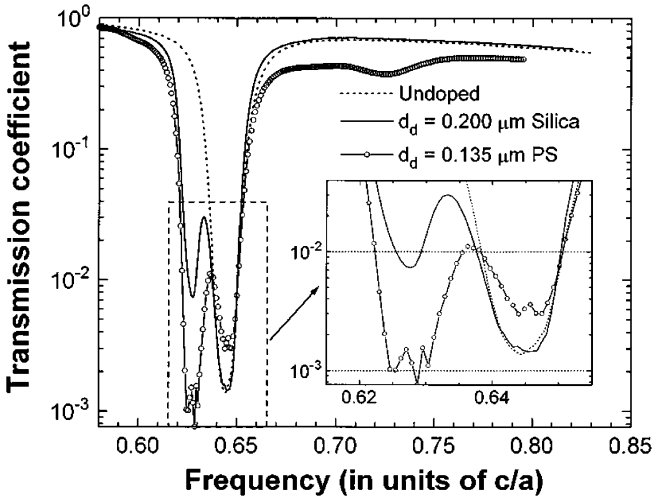

Figure 10. Near-IR transmission spectra for CCs containing intrinsic polystyrene donor impurities (10% number fraction) expressed in normalized frequency units (c/a). The host colloid diameter is 173 nm, the dopant colloids have diameters of 204, 214, and 222 nm. The dotted curve is collected from an undoped CC, the other curves are from doped CCs. Reproduced with permission from [106]. Copyright 1996 the American Physical Society.

ing impurity concentration in dried CCs, however distinguishable defect modes within the gap were not observed.[108,109]

Substitutional doping does not afford control of defect placement and can therefore only be used to create randomly distributed point defects. For the fabrication of more complex defect structures, required for many advanced functionalities, an external fabrication technique is necessary.

2D Embedded Defects via Multistep Procedures: Several multistep procedures have been developed for the fabrication of extrinsic point, linear, and planar defects within self-assembled PhCs. These approaches generally incorporate a 2D plane of defects sandwiched between two CCs. The procedure begins with the growth of a CC, followed by the deposition of an intermediate layer and perhaps 2D lithographic patterning of this layer, and is concluded with the growth of an overlying CC. Additional steps may include filling the interstitial space of the CC and template removal. In this fashion, embedded features of limited dimensionality can be defined within colloidal PhCs.

Through e-beam and nanoimprint lithography extrinsic point defects can be defined in or on CCs (Fig. 11). E-beam lithography was used to individually expose an array of spheres on the top layer of a CC and it was proposed that an additional CC could be grown before development to embed the defects.[110] Nanoimprint lithography was used to introduce a plane of point defects between two colloidal multilayers.[111] Alignment of defects with the CC lattice was not possible and multiple additional processing steps were required to embed the layer of defects; however, since nanoimprint lithography is a parallel, less time-consuming process than e-beam lithography, it may still find application. It will be interesting to compare the optical properties of a 2D embedded layer of extrinsic point defects with those from randomly three-dimensionally distributed intrinsic point defects introduced via substitutional doping (see previous section).

It is straightforward to extend e-beam and nanoimprint techniques to define linear and other 2D defects in CCs.[111–114] A similar approach to define embedded linear extrinsic defects is to use conventional photolithography to pattern a photoresist deposited on a CC (Fig. 12). Following the assembly of another crystal on this structure and removal of the photoresist, buried linear air defects have been incorporated within CCs.[115,116] While these linear defects have been suggested for use as waveguides, optics have only been measured normal to their long axis.[115] There is a report that measures transmission through "opal-clad" waveguides, however, in that case the waveguide is not completely surrounded by the CC.[117]

Another technique used to define extrinsic linear defects in CC-based PhCs is laser microannealing, which was used to write micrometer-scale defects on the surface of silicon inverse opals by inducing a localized phase transition from

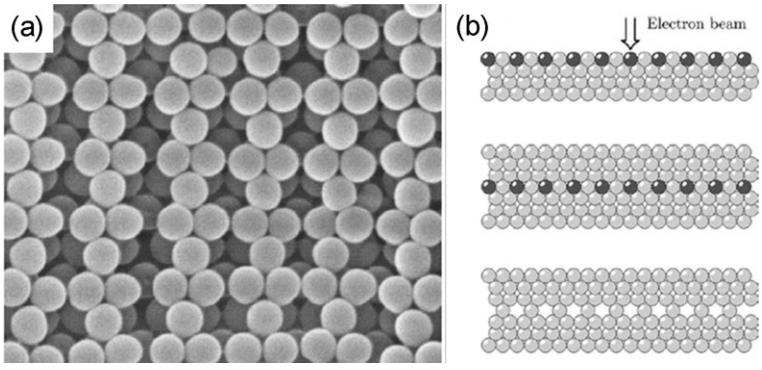

Figure 11. a) SEM image presenting a rectangular lattice of point defects defined on the surface of a PMMA CC (lattice parameter is 498 nm). b) Proposed process for embedding defects: 1. e-beam exposure, 2. growth of second CC, 3. development of exposed regions. Reproduced with permission from [110]. Copyright 2005 Elsevier.

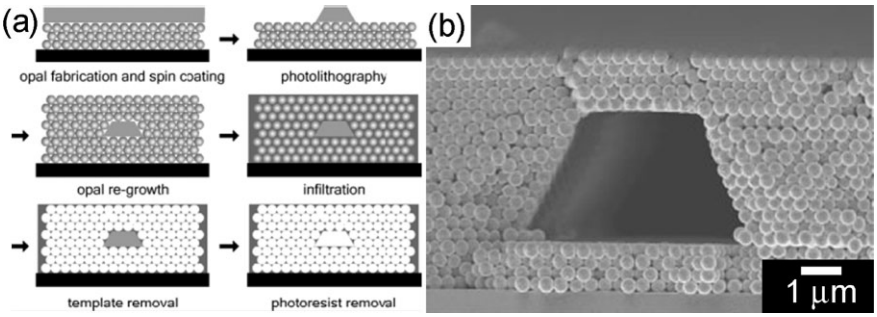

Figure 12. a) Schematic procedure for incorporating line defects within colloidal PhCs. b) SEM image of an air-core line defect, embedded within a silica CC. The boxes highlight the high-quality registration between the defect, original CC, and that grown via a second deposition. Similar results were concurrently obtained by Ozin and co-workers [115]. Reproduced from [116].

amorphous Si:H to nanocrystalline Si:H,[118] resulting in a lowering of the refractive index in the microannealed region from 4.00 to 3.85 (3.75 %). If the degree of crystallinity in the annealed region can be improved to yield a larger refractive-index change, and an approach developed to form an additional high-refractive-index inverse opal on top of the defined defect, laser microannealing may enable the definition of useful defects in silicon inverse opals.

Colvin and co-workers constructed colloidal superlattices with engineered midgap states via multiple depositions of colloidal layers with alternating colloid sizes.[119,120] Qualitative correspondence between normal incidence spectroscopy data and scalar wave approximation simulations supported the presence of superlattice effects (Fig. 13).[120] Similarly, Perfect consisting of TiO_2 nanoparticles has also been embedded in a CC through a similar process.[123]

soons and co-workers incorporated the first 2D embedded planar defect within a CC using a multistep colloidal growth process.[121,122] This structure consisted of two colloidal multilayers sandwiching an embedded monolayer of larger spheres. The colloidal multilayers were grown via vertical deposition, while a Langmuir–Blodgett technique was used to uniformly deposit the monolayer of larger spheres. Transmission measurements were used to confirm the presence of a defect mode within the pseudogap and establish the impact of monolayer thickness on the position of the defect mode.[121,122] A 2D planar de-

A multiple-step procedure for incorporating an extrinsic embedded planar defect consisting of a layer of silica between two silica–air inverse opals is shown in Figure 14.[124,125] The impact of the silica defect layer thickness on position of the defect mode within the pseudogap was studied experimentally[124–126] and via scalar wave approximation calculations.[125] The overall shape of the spectra agreed qualitatively, however a discrepancy was noted in the reflectance intensities and all theoretical spectra were scaled by an arbitrary factor to enable comparison.[125] Active planar embedded defects were incorporated into a CC via the growth or transfer printing of a polyelectrolyte multilayer on a CC followed by the

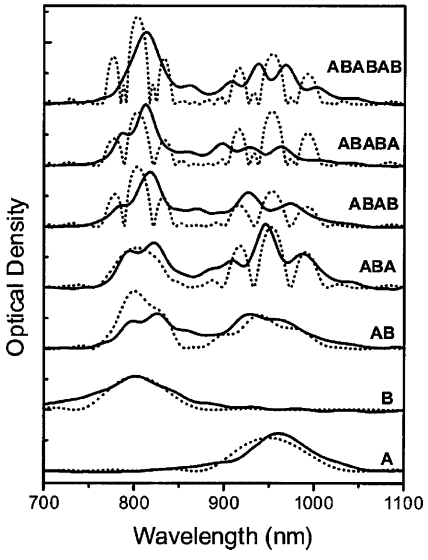

Figure 13. Experimental (solid) and simulated (dashed) spectroscopy from a series of CC superlattices deposited by alternating layers of microspheres (A spheres are 451 nm and B spheres are 381 nm). Spectra were simulated using the scalar-wave approximation and an overall multiplicative scaling was applied for each curve to facilitate comparison between experiment and theory. Reproduced with permission from [120]. Copyright 2001 the American Physical Society.

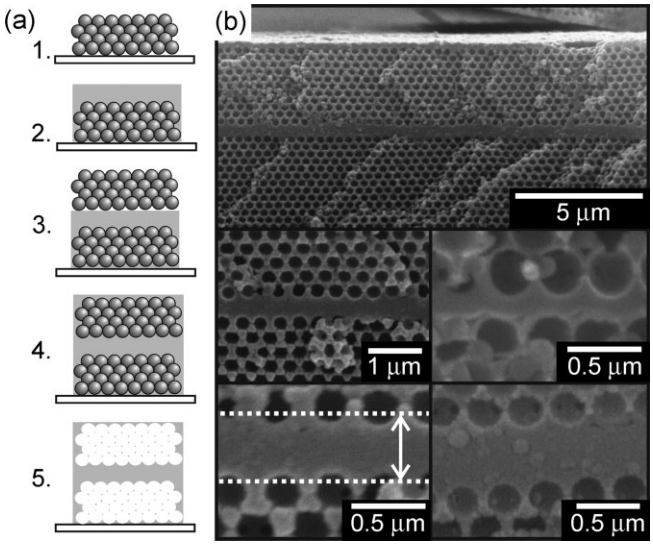

Figure 14. a) Schematic procedure for embedding planar defects in colloidal PhCs: 1. formation of polystyrene CC, 2. infiltration of CC with silica and growth of excess layer, 3. deposition of second polystyrene CC, 4. infiltration of second CC with silica, 5. removal of polystyrene. b) SEM image demonstrating the incorporation of silica planar defects with defined thicknesses within silica inverse opals. Sphere diameter is 375 ± 15 nm. Similar results were concurrently obtained by Lopez and co-workers [124]. Adapted from [125].

ADVANCED MATERIALS

subsequent growth of a second CC.[127] The polyelectrolyte multilayer swells in response to a chemical, optical, or thermal stimulus, which gives rise to a small but detectable shift in the position of the defect mode within the pseudogap.[127–129]

3D Embedded Defects via TPP: Although a number of approaches have been proposed for forming defects of limited dimensionality, to impart advanced functionalities, it is necessary to have a means to controllably incorporate complex pre-engineered defects with 3D spatial control. The first method for incorporating well-defined 3D defects within CCs was demonstrated by Braun and co-workers.[130]

This attractive technique employs TPP (for description, see Sec. 3.1.5) to fabricate high-resolution 3D embedded polymer features within CCs.[131] After infiltrating the CC with a two-photon polymerizable resin, a localized excitation volume is scanned throughout the material to expose the desired regions, defining high-resolution 3D embedded features (Fig. 15a and b). As described in Section 3.2.1, TPP can also be used to define features in PhCs formed by multibeam holography.[88]

TPP is an appealing method for writing defects within self-assembled or holographic PhCs for a number of reasons. TPP is a flexible technique capable of writing isolated, embedded, 3D features throughout the bulk of a crystal (on the order of 150 μm deep). Furthermore, TPP affords high resolution, with the smallest reported polymerizable volume element being an ellipsoid of 100 nm × ca. 300 nm.[132] When performed in conjunction with in situ fluorescence confocal imaging, it is possible to pinpoint the location of the TPP features with respect to the PhC lattice.[88]

An important consideration for any cPBG application is the ability to convert the PhC to a high-refractive-index structure that exhibits a cPBG. Generally, this is accomplished for colloidal PhCs through infiltration with a high-index material such as Si at an elevated temperature, followed by removal of the silica, resulting in an inverse opal structure. Here, both the TPP features and CC serve as a template for the final structure, resulting in a silicon–air inverse opal (which may possess a cPBG) containing embedded air defects. See Figures 15c and 16b for examples of defects in silicon-air inverse opals.[133] In the work presented in Figure 16, TPP was used to deposit a SiO_2 hybrid photoresist within a silica-based opal. After chemical vapor deposition (CVD) of Si and HF etching embedded hollow waveguide structures within a high-refractive-index inverse opal were formed. For success following this general procedure it is important that the materials formed through TPP are stable at the requisite high temperatures, for example, 250–350 °C for CVD of Si or Ge. Inorganic[133] or robust organic resins[134] deposited within silica CCs appear to be appropriate; the ceramic host appears to prevent deformation of polymer features at elevated temperatures.

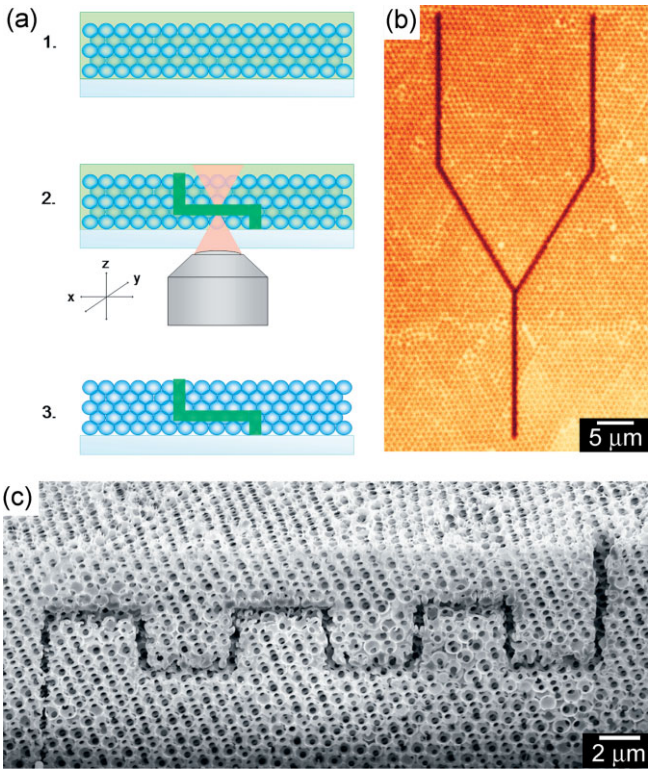

Figure 15. a) Schematic of experimental procedure for defining TPP embedded defects in silica colloidal PhCs, involving: 1. infiltration of CC with monomer, 2. TPP writing of desired features, 3. removal of unreacted monomer leaving behind CC containing an embedded feature. b) In situ fluorescence confocal microscopy image of a feature formed through TPP in a CC. c) SEM cross-sectional image of a TPP written air defect embedded within a silicon-air inverse opal [136].

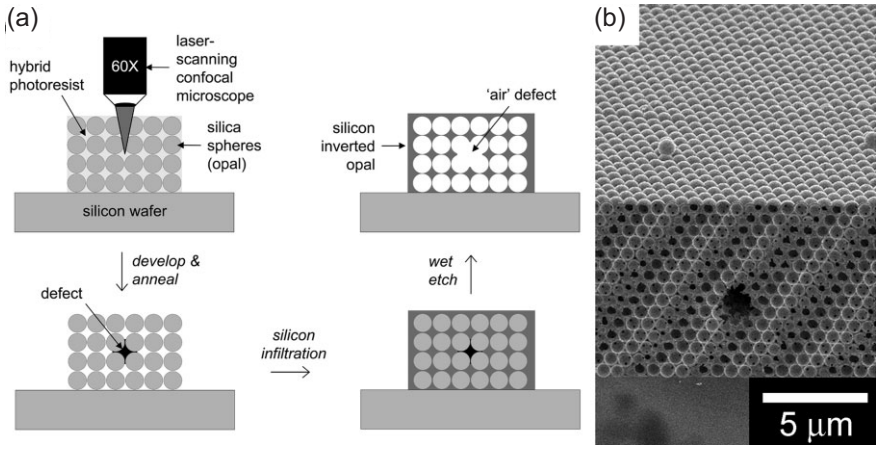

Figure 16. a) Schematic of experimental procedure for inverting a silica CC with embedded two-photon polymerized defects in silicon. b) Cross-sectional SEM image of a silicon inverse opal with an embedded air-core line defect with a diameter of approximately 1 μm. Adapted from [133].

TPP in CCs is a very flexible fabrication approach for the formation of complex structures, however, guidance for the design of optically interesting defects in colloidal PhCs is limited. The most notable effort to date on theory and computation of waveguide structures in CCs was recently published by Lousse and Fan, where it was proposed that coupled cavities are much more efficient for the guiding of light in an inverse opal based PC than simple tubelike defects.[135] Coupled cavities contain a much larger fraction of the light in the air voids, while simple tubelike guides concentrate most of the light in the walls of the tube, where scattering and other loss mechanisms are much more likely to operate.

4. Future Directions and Conclusions

Clearly, great strides have been made in the controlled incorporation of defects within 3D PhCs, extending their functionality and viability for PBG-based applications. Defects have been incorporated within 3D PhCs formed via most fabrication routes, including self-assembly, holography, controlled etching, and lithographic procedures. However, it is also clear that much work remains. To date, most defect structures are simple and there is only limited optical characterization. Also, with only a few exceptions, theory and simulation has primarily been used to explain observed results, not to guide experimental design. The development of reproducible techniques to mass produce high-quality 3D PhCs containing controlled defects will open the door to a new era where microphotonic devices will be combined with, or even replace current microelectronic devices.

Received: April 9, 2006
Published online: September 21, 2006

[1] K. Ohtaka, *Phys. Rev. B* **1979**, *19*, 5057.
[2] V. P. Bykov, *Sov. J. Quantum Electron.* **1975**, *4*, 861.
[3] E. Yablonovitch, *Phys. Rev. Lett.* **1987**, *58*, 2059.
[4] S. John, *Phys. Rev. Lett.* **1987**, *58*, 2486.
[5] C. Lopez, *Adv. Mater.* **2003**, *15*, 1679.
[6] R. D. Meade, A. Devenyi, J. D. Joannopoulos, O. L. Alerhand, D. A. Smith, K. Kash, *J. Appl. Phys.* **1994**, *75*, 4753.
[7] S. H. Fan, J. N. Winn, A. Devenyi, J. C. Chen, R. D. Meade, J. D. Joannopoulos, *J. Opt. Soc. Am. B* **1995**, *12*, 1267.
[8] A. Mekis, J. C. Chen, I. Kurland, S. H. Fan, P. R. Villeneuve, J. D. Joannopoulos, *Phys. Rev. Lett.* **1996**, *77*, 3787.
[9] S. John, T. Quang, *Phys. Rev. Lett.* **1997**, *78*, 1888.
[10] Y. Fink, J. N. Winn, S. H. Fan, C. P. Chen, J. Michel, J. D. Joannopoulos, E. L. Thomas, *Science* **1998**, *282*, 1679.
[11] P. Russell, *Science* **2003**, *299*, 358.
[12] S. Noda, K. Tomoda, N. Yamamoto, A. Chutinan, *Science* **2000**, *289*, 604.
[13] J. R. Wendt, G. A. Vawter, P. L. Gourley, T. M. Brennan, B. E. Hammons, *J. Vac. Sci. Technol. B* **1993**, *11*, 2637.
[14] A. Chutinan, S. John, O. Toader, *Phys. Rev. Lett.* **2003**, *90*, 3901.
[15] T. F. Krauss, R. M. De La Rue, S. Brand, *Nature* **1996**, *383*, 699.
[16] R. D. Meade, K. D. Brommer, A. M. Rappe, J. D. Joannopoulos, *Appl. Phys. Lett.* **1992**, *61*, 495.
[17] Y. N. Xia, G. M. Whitesides, *Annu. Rev. Mater. Sci.* **1998**, *28*, 153.
[18] S. Noda, A. Chutinan, M. Imada, *Nature* **2000**, *407*, 608.
[19] A. Birner, R. B. Wehrspohn, U. M. Gosele, K. Busch, *Adv. Mater.* **2001**, *13*, 377.
[20] B. S. Song, S. Noda, T. Asano, Y. Akahane, *Nat. Mater.* **2005**, *4*, 207.
[21] S. H. Fan, P. R. Villeneuve, J. D. Joannopoulos, H. A. Haus, *Opt. Express* **1998**, *3*, 4.
[22] H. Takano, B. S. Song, T. Asano, S. Noda, *Appl. Phys. Lett.* **2005**, *86*, 1101.
[23] S. H. Fan, S. G. Johnson, J. D. Joannopoulos, C. Manolatou, H. A. Haus, *J. Opt. Soc. Am. B* **2001**, *18*, 162.
[24] O. Painter, R. K. Lee, A. Scherer, A. Yariv, J. D. O'Brien, P. D. Dapkus, I. Kim, *Science* **1999**, *284*, 1819.
[25] M. Fujita, S. Takahashi, Y. Tanaka, T. Asano, S. Noda, *Science* **2005**, *308*, 1296.
[26] T. Yoshie, A. Scherer, J. Hendrickson, G. Khitrova, H. M. Gibbs, G. Rupper, C. Ell, O. B. Shchekin, D. G. Deppe, *Nature* **2004**, *432*, 200.
[27] K. M. Ho, C. T. Chan, C. M. Soukoulis, R. Biswas, M. Sigalas, *Solid State Commun.* **1994**, *89*, 413.
[28] N. Yamamoto, S. Noda, A. Chutinan, *Jpn. J. Appl. Phys. Part 2* **1998**, *37*, L1052.
[29] A. Chutinan, S. Noda, *Appl. Phys. Lett.* **1999**, *75*, 3739.
[30] S.-Y. Lin, J. G. Fleming, D. L. Hetherington, B. K. Smith, R. Biswas, K. M. Ho, M. M. Sigalas, W. Zubrzycki, S. R. Kurth, J. Bur, *Nature* **1998**, *394*, 251.
[31] M. H. Qi, E. Lidorikis, P. T. Rakich, S. G. Johnson, J. D. Joannopoulos, E. P. Ippen, H. I. Smith, *Nature* **2004**, *429*, 538.
[32] K. Sakoda, H. Shiroma, *Phys. Rev. B* **1997**, *56*, 4830.
[33] V. Lehmann, *J. Electrochem. Soc.* **1993**, *140*, 2836.
[34] U. Gruning, V. Lehmann, C. M. Engelhardt, *Appl. Phys. Lett.* **1995**, *66*, 3254.
[35] F. Muller, A. Birner, J. Schilling, U. Gosele, C. Kettner, P. Hanggi, *Phys. Status Solidi A* **2000**, *182*, 585.
[36] J. Schilling, F. Muller, S. Matthias, R. B. Wehrspohn, U. Gosele, K. Busch, *Appl. Phys. Lett.* **2001**, *78*, 1180.
[37] H. A. Lopez, P. M. Fauchet, *Appl. Phys. Lett.* **2000**, *77*, 3704.
[38] S. Matthias, F. Muller, J. Schilling, U. Gosele, *Appl. Phys. A* **2005**, *80*, 1391.
[39] G. Mertens, R. B. Wehrspohn, H. S. Kitzerow, S. Matthias, C. Jamois, U. Gosele, *Appl. Phys. Lett.* **2005**, *87*, 1108.
[40] S. Matthias, F. Muller, C. Jamois, R. B. Wehrspohn, U. Gosele, *Adv. Mater.* **2004**, *16*, 2166.
[41] J. Schilling, J. White, A. Scherer, G. Stupian, R. Hillebrand, U. Gosele, *Appl. Phys. Lett.* **2005**, *86*, 1101.
[42] S. R. Kennedy, M. J. Brett, O. Toader, S. John, *Nano Lett.* **2002**, *2*, 59.
[43] O. Toader, S. John, *Science* **2001**, *292*, 1133.
[44] O. Toader, S. John, *Phys. Rev. E: Stat. Phys., Plasmas, Fluids, Relat. Interdiscip. Top.* **2002**, *66*, 016 610.
[45] A. C. van Popta, M. J. Brett, J. C. Sit, *J. Appl. Phys.* **2005**, *98*, 3517.
[46] M. O. Jensen, M. J. Brett, *Nanotechnology* **2005**, *16*, 2639.
[47] M. O. Jensen, M. J. Brett, *J. Nanosci. Nanotechnol.* **2005**, *5*, 723.
[48] H. Morishita, Y. Hatamura, in *Proc. IEEE/RSJ Int. Conf. Intelligent Robots and Systems*, Yokohama, Japan, July 26–30, **1993**.
[49] F. Garcia-Santamaria, H. T. Miyazaki, A. Urquia, M. Ibisate, M. Belmonte, N. Shinya, F. Meseguer, C. Lopez, *Adv. Mater.* **2002**, *14*, 1144.
[50] F. Garcia-Santamaria, C. Lopez, F. Meseguer, F. Lopez-Tejeira, J. Sanchez-Dehesa, H. T. Miyazaki, *Appl. Phys. Lett.* **2001**, *79*, 2309.
[51] K. Aoki, H. T. Miyazaki, H. Hirayama, K. Inoshita, T. Baba, K. Sakoda, N. Shinya, Y. Aoyagi, *Nat. Mater.* **2003**, *2*, 117.
[52] D. L. J. Vossen, A. van der Horst, M. Dogterom, A. van Blaaderen, *Rev. Sci. Instrum.* **2004**, *75*, 2960.
[53] A. van Blaaderen, J. P. Hoogenboom, D. L. J. Vossen, A. Yethiraj, A. van der Horst, K. Visscher, M. Dogterom, *Faraday Discuss.* **2003**, *123*, 107.
[54] T. Kasaya, H. T. Miyazaki, S. Saito, K. Koyano, T. Yamaura, T. Sato, *Rev. Sci. Instrum.* **2004**, *75*, 2033.

[55] G. M. Gratson, F. Garcia-Santamaria, V. Lousse, M. Xu, S. H. Fan, J. A. Lewis, P. V. Braun, *Adv. Mater.* **2006**, *18*, 461.
[56] N. Tétreault, G. von Freymann, M. Deubel, M. Hermatschweiler, F. Pérez-Willard, S. John, M. Wegener, G. A. Ozin, *Adv. Mater.* **2006**, *18*, 457.
[57] G. M. Gratson, M. J. Xu, J. A. Lewis, *Nature* **2004**, *428*, 386.
[58] G. M. Gratson, *Ph.D. Thesis*, University of Illinois at Urbana-Champaign, Urbana **2005**.
[59] H. B. Sun, S. Matsuo, H. Misawa, *Appl. Phys. Lett.* **1999**, *74*, 786.
[60] J. E. Smay, J. Cesarano, J. A. Lewis, *Langmuir* **2002**, *18*, 5429.
[61] H. S. Sozuer, J. P. Dowling, *J. Mod. Opt.* **1994**, *41*, 231.
[62] J. H. Strickler, W. W. Webb, *Proc. SPIE-Int. Soc. Opt. Eng.* **1990**, *1398*, 107.
[63] J. D. Pitts, P. J. Campagnola, G. A. Epling, S. L. Goodman, *Macromolecules* **2000**, *33*, 1514.
[64] W. H. Zhou, S. M. Kuebler, K. L. Braun, T. Y. Yu, J. K. Cammack, C. K. Ober, J. W. Perry, S. R. Marder, *Science* **2002**, *296*, 1106.
[65] T. Y. Yu, C. K. Ober, S. M. Kuebler, W. H. Zhou, S. R. Marder, J. W. Perry, *Adv. Mater.* **2003**, *15*, 517.
[66] T. Watanabe, M. Akiyama, K. Totani, S. M. Kuebler, F. Stellacci, W. Wenseleers, K. Braun, S. R. Marder, J. W. Perry, *Adv. Funct. Mater.* **2002**, *12*, 611.
[67] B. H. Cumpston, S. P. Ananthavel, S. Barlow, D. L. Dyer, J. E. Ehrlich, L. L. Erskine, A. A. Heikal, S. M. Kuebler, I. Y. S. Lee, D. McCord-Maughon, J. Q. Qin, H. Rockel, M. Rumi, X. L. Wu, S. R. Marder, J. W. Perry, *Nature* **1999**, *398*, 51.
[68] Z. Bayindir, Y. Sun, M. J. Naughton, C. N. LaFratta, T. Baldacchini, J. T. Fourkas, J. Stewart, B. E. A. Saleh, M. C. Teich, *Appl. Phys. Lett.* **2005**, *86*, 4105.
[69] T. Tanaka, H. B. Sun, S. Kawata, *Appl. Phys. Lett.* **2002**, *80*, 312.
[70] H. B. Sun, T. Kawakami, Y. Xu, J.-Y. Ye, S. Matuso, H. Misawa, M. Miwa, R. Kaneko, *Opt. Lett.* **2000**, *25*, 1110.
[71] H. B. Sun, K. Takada, S. Kawata, *Appl. Phys. Lett.* **2001**, *79*, 3173.
[72] J. M. Kim, H. Muramatsu, *Nano Lett.* **2005**, *5*, 309.
[73] R. A. Borisov, G. N. Dorojkina, N. I. Koroteev, V. M. Kozenkov, S. A. Magnitskii, D. V. Malakhov, A. V. Tarasishin, A. M. Zheltikov, *Appl. Phys. B* **1998**, *67*, 765.
[74] R. A. Borisov, G. N. Dorojkina, N. I. Koroteev, V. M. Kozenkov, S. A. Magnitskii, D. V. Malakhov, A. V. Tarasishin, A. M. Zheltikov, *Laser Phys.* **1998**, *8*, 1105.
[75] M. Straub, M. Gu, *Opt. Lett.* **2002**, *27*, 1824.
[76] J. Serbin, A. Egbert, A. Ostendorf, B. N. Chichkov, R. Houbertz, G. Domann, J. Schulz, C. Cronauer, L. Frohlich, M. Popall, *Opt. Lett.* **2003**, *28*, 301.
[77] K. Kaneko, H. B. Sun, X. M. Duan, S. Kawata, *Appl. Phys. Lett.* **2003**, *83*, 2091.
[78] M. Deubel, G. von Freymann, M. Wegener, S. Pereira, K. Busch, C. M. Soukoulis, *Nat. Mater.* **2004**, *3*, 444.
[79] M. Deubel, M. Wegener, A. Kaso, S. John, *Appl. Phys. Lett.* **2004**, *85*, 1895.
[80] J. Serbin, A. Ovsianikov, B. Chichkov, *Opt. Express* **2004**, *12*, 5221.
[81] L. H. Nguyen, M. Straub, M. Gu, *Adv. Funct. Mater.* **2005**, *15*, 209.
[82] O. Toader, M. Berciu, S. John, *Phys. Rev. Lett.* **2003**, *90*, 233 901.
[83] S. Wong, M. Deubel, F. Pérez-Willard, S. John, G. A. Ozin, M. Wegener, G. von Freymann, *Adv. Mater.* **2006**, *18*, 265.
[84] V. Berger, O. GauthierLafaye, E. Costard, *J. Appl. Phys.* **1997**, *82*, 60.
[85] M. Campbell, D. N. Sharp, M. T. Harrison, R. G. Denning, A. J. Turberfield, *Nature* **2000**, *404*, 53.
[86] K. Y. Lee, N. LaBianca, S. A. Rishton, S. Zolgharnain, J. D. Gelorme, J. Shaw, T. H. P. Chang, *J. Vac. Sci. Technol. B* **1995**, *13*, 3012.
[87] N. D. Lai, W. P. Liang, J. H. Lin, C. C. Hsu, *Opt. Express* **2005**, *13*, 5331.
[88] J. Scrimgeour, D. N. Sharp, C. F. Blanford, O. M. Roche, R. G. Denning, A. J. Turberfield, *Adv. Mater.* **2006**, *12*, 1557.
[89] Y. V. Miklyaev, D. C. Meisel, A. Blanco, G. von Freymann, K. Busch, W. Koch, C. Enkrich, M. Deubel, M. Wegener, *Appl. Phys. Lett.* **2003**, *82*, 1284.
[90] J. H. Moon, S. Yang, D. J. Pine, S. M. Yang, *Opt. Express* **2005**, *13*, 9841.
[91] Y. K. Pang, J. C. W. Lee, H. F. Lee, W. Y. Tam, C. T. Chan, P. Sheng, *Opt. Express* **2005**, *13*, 7615.
[92] J. S. King, E. Graugnard, O. M. Roche, D. N. Sharp, J. Scrimgeour, R. G. Denning, A. J. Turberfield, C. J. Summers, *Adv. Mater.* **2006**, *12*, 1561.
[93] S. Yang, M. Megens, J. Aizenberg, P. Wiltzius, P. M. Chaikin, W. B. Russel, *Chem. Mater.* **2002**, *14*, 2831.
[94] S. Jeon, J. U. Park, R. Cirelli, S. Yang, C. E. Heitzman, P. V. Braun, P. J. A. Kenis, J. A. Rogers, *Proc. Natl. Acad. Sci. USA* **2004**, *101*, 12 428.
[95] W. Ehrfeld, A. Schmidt, *J. Vac. Sci. Technol. B* **1998**, *16*, 3526.
[96] G. Feiertag, W. Ehrfeld, H. Freimuth, H. Kolle, H. Lehr, M. Schmidt, M. M. Sigalas, C. M. Soukoulis, G. Kiriakidis, T. Pedersen, J. Kuhl, W. Koenig, *Appl. Phys. Lett.* **1997**, *71*, 1441.
[97] C. Cuisin, A. Chelnokov, J. M. Lourtioz, D. Decanini, Y. Chen, *J. Vac. Sci. Technol. B* **2000**, *18*, 3505.
[98] E. Yablonovitch, T. J. Gmitter, K. M. Leung, *Phys. Rev. Lett.* **1991**, *67*, 2295.
[99] C. Cuisin, A. Chelnokov, J. M. Lourtioz, D. Decanini, Y. Chen, *Appl. Phys. Lett.* **2000**, *77*, 770.
[100] C. Cuisin, A. Chelnokov, D. Decanini, D. Peyrade, Y. Chen, J. M. Lourtioz, *Opt. Quantum Electron.* **2002**, *34*, 13.
[101] M. Tormen, L. Businaro, M. Altissimo, F. Romanato, S. Cabrini, F. Perennes, R. Proietti, H. B. Sun, S. Kawata, E. Di Fabrizio, *Microelectron. Eng.* **2004**, *73–74*, 535.
[102] F. Romanato, R. Kumar, E. Di Fabrizio, *Nanotechnology* **2005**, *16*, 40.
[103] A. P. Philipse, *J. Mater. Sci. Lett.* **1989**, *8*, 1371.
[104] O. D. Velev, T. A. Jede, R. F. Lobo, A. M. Lenhoff, *Nature* **1997**, *389*, 447.
[105] H. S. Sozuer, J. W. Haus, R. Inguva, *Phys. Rev. B* **1992**, *45*, 13 962.
[106] R. D. Pradhan, I. I. Tarhan, G. H. Watson, *Phys. Rev. B* **1996**, *54*, 13 721.
[107] J. B. Pendry, A. Mackinnon, *Phys. Rev. Lett.* **1992**, *69*, 2772.
[108] B. Gates, Y. Xia, *Appl. Phys. Lett.* **2001**, *78*, 3178.
[109] E. Palacios-Lidon, B. H. Juarez, E. Castillo-Martinez, C. Lopez, *J. Appl. Phys.* **2005**, *97*, 063 502.
[110] F. Jonsson, C. M. S. Torres, J. Seekamp, M. Schniedergers, A. Tiedemann, J. H. Ye, R. Zentel, *Microelectron. Eng.* **2005**, *78–79*, 429.
[111] Q. F. Yan, A. Chen, S. J. Chua, X. S. Zhao, *Adv. Mater.* **2005**, *17*, 2849.
[112] P. Ferrand, M. Egen, R. Zentel, J. Seekamp, S. G. Romanov, C. M. S. Torres, *Appl. Phys. Lett.* **2003**, *83*, 5289.
[113] P. Ferrand, J. Seekamp, M. Egen, R. Zentel, S. G. Romanov, C. M. S. Torres, *Microelectron. Eng.* **2004**, *73–74*, 362.
[114] B. H. Juarez, D. Golmayo, P. A. Postigo, C. Lopez, *Adv. Mater* **2004**, *16*, 1732.
[115] E. Vekris, V. Kitaev, G. von Freymann, D. D. Perovic, J. S. Aitchison, G. A. Ozin, *Adv. Mater* **2005**, *17*, 1269.
[116] Q. F. Yan, Z. C. Zhou, X. S. Zhao, S. J. Chua, *Adv. Mater.* **2005**, *17*, 1917.
[117] K. H. Baek, A. Gopinath, *IEEE Photon. Technol. Lett.* **2005**, *17*, 351.
[118] N. Tetreault, H. Miguez, S. M. Yang, V. Kitaev, G. A. Ozin, *Adv. Mater.* **2003**, *15*, 1167.
[119] P. Jiang, G. N. Ostojic, R. Narat, D. M. Mittleman, V. L. Colvin, *Adv. Mater.* **2001**, *13*, 389.
[120] R. Rengarajan, P. Jiang, D. C. Larrabee, V. L. Colvin, D. M. Mittleman, *Phys. Rev. B* **2001**, *64*, 205 103.
[121] K. Wostyn, Y. X. Zhao, G. de Schaetzen, L. Hellemans, N. Matsuda, K. Clays, A. Persoons, *Langmuir* **2003**, *19*, 4465.

[122] Y. X. Zhao, K. Wostyn, G. de Schaetzen, K. Clays, L. Hellemans, A. Persoons, M. Szekeres, R. A. Schoonheydt, *Appl. Phys. Lett.* **2003**, *82*, 3764.
[123] R. Pozas, A. Mihi, M. Ocaña, H. Míguez, *Adv. Mater.* **2006**, *18*, 1183–1187.
[124] E. Palacios-Lidon, J. F. Galisteo-Lopez, B. H. Juarez, C. Lopez, *Adv. Mater.* **2004**, *16*, 341.
[125] N. Tetreault, A. Mihi, H. Miguez, I. Rodriguez, G. A. Ozin, F. Meseguer, V. Kitaev, *Adv. Mater.* **2004**, *16*, 346.
[126] L. K. Wang, Q. F. Yan, X. S. Zhao, *Langmuir* **2006**, *22*, 3481.
[127] N. Tetreault, A. C. Arsenault, A. Mihi, S. Wong, V. Kitaev, I. Manners, H. Miguez, G. A. Ozin, *Adv. Mater.* **2005**, *17*, 1912.
[128] F. Fleischhaker, A. C. Arsenault, V. Kitaev, F. C. Peiris, G. von Freymann, I. Manners, R. Zentel, G. A. Ozin, *J. Am. Chem. Soc.* **2005**, *127*, 9318.
[129] F. Fleischhaker, A. C. Arsenault, Z. Wang, V. Kitaev, F. C. Peiris, G. von Freymann, I. Manners, R. Zentel, G. A. Ozin, *Adv. Mater.* **2005**, *17*, 2455.
[130] W. M. Lee, S. A. Pruzinsky, P. V. Braun, *Adv. Mater.* **2002**, *14*, 271.
[131] S. A. Pruzinsky, P. V. Braun, *Adv. Funct. Mater.* **2005**, *15*, 1995.
[132] K. Takada, H. B. Sun, S. Kawata, *Appl. Phys. Lett.* **2005**, *86*, 71 122.
[133] Y. H. Jun, C. A. Leatherdale, D. J. Norris, *Adv. Mater.* **2005**, *17*, 1908.
[134] P. V. Braun, S. A. Pruzinsky, W. Lee, *Abstr. Pap. Am. Chem. Soc.* **2005**, *229*, U1113.
[135] V. Lousse, S. H. Fan, *Opt. Express* **2006**, *14*, 866.
[136] S. A. Pruzinsky, *Ph.D. Thesis*, University of Illinois at Urbana-Champaign, Urbana **2006**.